

ORAI3 contributes to hypoxia-inducible factor 1/2 α -sensitive colon cell migration

D. ZHU^{1,3}, R. HE², W. YU¹, C. LI⁴, H. CHENG¹, B. ZHU¹ and J. YAN^{1*} 

¹ Department of Physiology, Jining Medical University, Jining, Shandong, China

² School of International Education, Xinxiang Medical University, Xinxiang, Henan, China

³ Department of Urology Surgery, The First People's Hospital of Shangqiu, Shangqiu, Henan, China

⁴ Department of Physiology, Zhengzhou University, Zhengzhou, Henan, China

Received: August 30, 2020 • Accepted: December 29, 2020

Published online: June 22, 2021

© 2020 Akadémiai Kiadó, Budapest



ABSTRACT

Background: Hypoxia is a pivotal initiator of tumor angiogenesis and growth through the stabilization of hypoxia-inducible factors (HIFs). This study set out to examine the involvement of HIF-1 α and HIF-2 α in colon cancer and ascertained whether ORAI3 was involved in the pathway. **Materials and methods:** Patients and murine models as well as human colorectal adenocarcinoma tumor (CW2) cells were included to examine the levels of ORAI1/3 and HIF-1/2 α levels. Calcium imaging was utilized to ascertain the activity of calcium channel. Scratch assay was used to assess the migration capacity of the cells. **Results:** Tumors from murine colon cancer xenograft models and patients with colon cancer displayed high ORAI1/3 and HIF-1/2 α levels. Hypoxia treatment, mimicking the tumor microenvironment in vitro, increased ORAI1/3 and HIF-1/2 α expression as well as store-operated Ca²⁺ entry (SOCE). Of note is that HIF-1/2 α silencing decreased SOCE, and HIF-1/2 α overexpression facilitated SOCE. Furthermore, ORAI3 rather than ORAI1 expression was inhibited by HIF-1/2 α silencing while increased by ML228. Luciferase assay also confirmed that ORAI3 was elevated in the presence of ML228, indicating the linkage between HIF-1/2 α and ORAI3. Additionally, colony-forming potential and cell migration capacity were decreased in *siHIF-1 α* and *siHIF-2 α* as well as *siORAI3* cells, and the facilitating effect of ML228 on cell migration and colony-forming potential was also decreased in *siORAI3* CW-2 cells, which points out the importance of ORAI3 in HIF1/2 α pathway. **Conclusion:** Our findings allow to conclude that both HIF-1 α and HIF-2 α facilitate ORAI3 expression, hence enhancing colon cancer progression.

* Corresponding author. Department of Physiology, Jining Medical University, 133 Hehua Rd, 272067, Jining, Shandong, China. Fax: +8605373616019. E-mail: yanjing102@mail.jnmc.edu.cn

KEYWORDS

store-operated Ca^{2+} entry, ORAI3, colon cancer, HIF1/2 α

INTRODUCTION

Solid tumor tissue is often hypoxic due to the limited supporting capacity of normal tissue vasculature. Activation of hypoxia-inducible factors (HIFs) is the major pathway adopted by hypoxic cells in the tumor microenvironment, and is of great importance for tumor angiogenesis as well as growth [1]. HIFs are heterodimeric basic helix-loop-helix (bHLH)/Per-ARNT-Sim (PAS) transcription factor complexes, and are composed of an oxygen-labile α -subunit (HIF α) and a constitutively expressed β -subunit [2]. Stabilization of HIF α in response to hypoxia activates HIF complexes and results in the rapid accumulation of proteins needed for oxygen delivery [3]. HIF-1 α and HIF-2 α , the main drivers of the cellular response to low oxygen, are involved in the poor outcome of tumors [4–6].

Intracellular calcium (Ca^{2+}) concentration contributes to the orchestration of many cellular functions, including cell cycle progression and cell migration that are essential for cancer formation [7–9]. Store-operated Ca^{2+} channel (SOCC) is the primary pathway for Ca^{2+} influx in cancer cells, which is mainly activated by Ca^{2+} release from intracellular stores and triggered physiologically through stimulation of a wide variety of surface receptors. SOCC is accomplished by the pore-forming Ca^{2+} channel subunits calcium release-activated calcium channel protein (ORAI) 1, ORAI2, and ORAI3 [9–11] as well as their regulators, stromal interaction molecule (STIM) 1 and STIM2 [12, 13]. The reduction of store-operated Ca^{2+} entry (SOCE) inhibits the metastasis of breast, esophageal, cervical and prostate tumors [14–18]. As the major components of SOCC, ORAI1 and STIM1 are closely related to poor clinical outcomes in gastric and colorectal cancers [19, 20]. Meanwhile, emerging evidence shows that ORAI3 is also involved in carcinoma, including breast and prostate as well as lung cancer [21–23]. Noteworthy is that SOCC in estrogen receptor α -expressing (ER α^+) breast cancer cells is mediated by ORAI3 instead of the canonical ORAI1 pathway [24]. Besides, Azimi et al. reported the elevated ORAI3 level in breast cancer cells under hypoxia and confirmed the involvement of HIF-1 α [25], underlying the merge of HIF-1 α and ORAI3 in carcinogenesis. HIF-1 α is the best known and most widely described isoform, whereas the expression of HIF-2 α is restricted to the lung, heart and gut [26]. Yet for the overexpression of HIF-2 α in colorectal cancer [27, 28] the functions and related mechanism of HIF-2 α in cancer remain elusive. Here, we established the colon cancer model and used molecular approaches to address the relationship between HIF1/2 α and ORAI3 in the context of colon carcinogenesis.

MATERIALS AND METHODS**Ethics statement**

The protocols and the use of animals were approved by Jining Medical University and Xinxiang Medical University Animal Care and Use Committee.



Patients' samples

Tumor samples from 32 patients with colon cancer were collected between September 2019 and March 2020 at the First People's Hospital of Shangqiu (China). All patients gave written informed consent. Written informed consent was obtained from all patients who participated in the study, and the study was approved by the First People's Hospital of Shangqiu Ethics Review Board.

Cell culture and drugs

Experiments were performed in CW-2 (Procell, China) carcinoma cells grown in DMEM media (Sigma, USA), containing 10% fetal calf serum (Gibco) and 1% antibiotic/antimycotic solution. For hypoxia treatment, cells were subjected to hypoxia (1% O₂) for 12 h in a humidified hypoxia chamber (Stem Cell Technology, USA). Control cells were cultured in normoxic condition (5% CO₂).

ML228 (MedChemExpress), a potent HIF pathway activator[29] and was administered at 5 μ M.

The Orai3 knockdown plasmid was constructed using a lentivirus/GV248 plasmid (hU6-MCS-Ubiquitin-EGFP-IRES-puromycin) (Byotime) with an insert of shRNA (CCGGTGTG-GCCTTTGCCCTGCATTTCTCGAGAAATGCAGGGCAAAGGCCACATTTTTTG) targeting human Orai3. The shRNA virus and the negative control virus were packaged into HEK293T cells, and the titers were evaluated. The viruses were used to infect CW-2 cells. The stable transfected cells were selected using puromycin (10 μ g/mL).

For silencing, 1×10^5 cells were seeded 24 h before the experiment in antibiotic-free medium. Cells were transfected with 5 μ L/1000 μ L ON-TARGETplus Human Orai3 siRNA (5 μ M, Thermo Fisher Scientific) and ON-TARGETplus Human Hif-1/2 α siRNA (5 μ M) as well as ON-TARGETplus Non-targeting siRNA (5 μ M) using the cationic lipid DharmaFECT 1 transfection reagent (0.5 μ L/1000 μ L) according to the manufacturer's protocol. Cells were collected 24 h after transfection. To confirm the silencing efficiency, transcript levels were quantified by Western blotting and RT-PCR (Figs 1 and 3).

For overexpression, a Hif-1/2 α overexpression plasmid was constructed by inserting human Hif-1/2 α cDNA into a lentivirus/GV358 plasmid (GeneChem). The expression virus and lentivirus/GV358 were packaged into HEK293T cells, and the viruses were used to infect CW-2 cells.

Western blotting

Protein was separated by SDS-PAGE, thereafter transferred to PVDF membrane and blocked in 5% non-fat milk at room temperature for 1 h. Membranes were probed overnight at 4 °C with polyclonal rabbit anti-ORAI1 (1:1000, Abcam), anti-ORAI2 (1:1000, Abcam), anti-ORAI3 (1:1000, Abcam), HIF-2 α (1:1000, cell signaling), HIF-1 α (1:1000, cell signaling). After incubation with horseradish peroxidase-conjugated anti-rabbit secondary antibody (1:2000, Sigma) for 1 h at room temperature, the bands were visualized with enhanced chemiluminescence reagents (Sigma). Membranes were probed with GAPDH antibody as the loading control.

Real-time PCR

Total RNA was extracted from cells in TriFast (Peqlab). After DNase digestion, reverse transcription of total RNA was performed using Transcriptor High Fidelity cDNA Synthesis Kit



(Roche). Real-time polymerase chain reactions (RT-PCR) of the respective genes were set up in a total volume of 20 μ L using 40 ng of cDNA, 500 nM forward and reverse primer and 2 \times GoTaq qPCR Master Mix (Promega). Cycling conditions were as follows: 95 $^{\circ}$ C for 5 min, followed by 40 cycles of 58 $^{\circ}$ C for 30 s and 72 $^{\circ}$ C for 20 s.

The following primers were used (5' > 3'):

For *Orai1*:

Fw: GGTAGCGATGGTGGAAGTC; Rev: GACCGAGTTGAGGTTGTGG

For *Orai2*:

Fw CGTCTAACCACCATTCGG; Rev: CAAACAGATGCACGGCTA

For *Orai3*:

Fw: GCGGCTACCTGGACCTTA; Rev: TTGCTCACGGCTTCAATAT

For *Hif-1 α* :

Fw: CAGCCAGCAAGTCCTTCTGA; Rev: GGAGGGCTTGGAGAATTGCT

For *Hif-2 α* :

Fw: TTGCTTATTGGTGTGCTGCC; Rev: CAACATTCCCACACACTGCAG

For *Tbp* (TATA-box binding protein):

Fw: ACTCCTGCCACACCAGCC; Rev: GGTCAAGTTTACAGCCAAGATTCA

The specificity of PCR products was confirmed by analysis of a melting curve. Real-time PCR amplifications were performed on a CFX96 Real-Time System (Bio-Rad). *Tbp* was amplified to standardize the amount of sample RNA. Relative quantification of gene expression was achieved using the Δ CT method.

Luciferase reporter assay

The ORAI3 promoter containing the indicated sequences was inserted into the pGL3-Enhancer plasmid (Promega).

HRE1:AGGCGTGA

HRE2:GGAGGTGC

HRE3:GCATGTGC

HRE4:GTACGTGG

Then CW-2 cells were then co-transfected with the pGL3-ORAI3-3'-UTR and Renilla plasmid using Lipofectamine 2000 (Invitrogen) in the presence of ML228. 48 h after transfection, cell lysates were used for detecting firefly luciferase and Renilla luciferase activities using the luciferase reporter gene assay kit (Promega). The ratio of firefly to Renilla luciferase activity was used to express luciferase activities.

Ca²⁺ measurements

Cells were loaded with Fura-2/AM (1 μ M, Invitrogen) for 15 min at 37 $^{\circ}$ C. Cells were excited alternatively at 340 nm and 380 nm. Emitted fluorescence intensity was recorded at 505 nm. Data were acquired using Metafluor. Cytosolic Ca²⁺ concentration was estimated from the 340 nm/380 nm ratio. SOCE was determined by extracellular Ca²⁺ removal and subsequent Ca²⁺ re-addition in the presence of sarco-/endoplasmic reticulum Ca²⁺/ATPase (SERCA) inhibitor thapsigargin (1 μ M, Invitrogen). The slope (delta ratio/s) represents the velocity of elevated [Ca²⁺]_i and peak (delta ratio) represents the amplitude of elevated [Ca²⁺]_i.



Scratch assay

CW-2 cells were seeded in a 6-well plate (NEST Biotechnology) and incubated until they reached confluent monolayer. The monolayer was wounded using a 200 μ L pipette tip. The movement of cells in the scratched area is photographically monitored at 0 and 24 h after treatment. The percentage of scratch coverage of cells was measured.

Colony formation assay

Single-cell suspension (10^5) of CW-2 cells was seeded into 6-well plates under hypoxia. Then cells were allowed to grow for 10 days under hypoxia. To visualize colonies, cells were fixed with methanol and stained with 0.5% crystal violet. Colonies with ≥ 50 cells were manually quantified.

$$\text{Colony formation rate} = (\text{colonies numbers}) / (\text{number of planted cells}) \times 100\%$$

Murine colon cancer xenograft models

Thymic NCr-nu/nu mice, 6 weeks of age with an average body weight of 20 g, were obtained from Beijing Vital River Laboratory Animal Technology Company. CW-2 cells (10^7 cells) were implanted in the left flank of each nude mouse. Sodium chloride was used as vehicle controls. Tumor sizes were measured twice weekly after initial detection. Tumor volume was calculated using the formula: tumor volume (mm^3) = length \times width \times height \times 3.14/6. On day 21, the animals were sacrificed, and the subcutaneous tumors were harvested.

Stable Orai3 knockdown cells (shRNA-Orai3) and vector control cells (NC) were injected into the flanks of nude mice. Mice were sacrificed in 25 days, and cancer formation was examined.

Statistics

Data are provided as means \pm SEM, n represents the number of independent experiments. All data were tested for significance using unpaired Student *t*-test. Only results with $p < 0.05$ were considered statistically significant.

RESULTS

High expression of ORAI1/3 and HIF1/2 α in colon cancer

By establishing colon cancer xenograft models, we confirmed the enhanced expression of ORAI1/3 and HIF-1/2 α in the tumor tissue as compared with the healthy colon tissues (Fig. 1A and B). Consistently, tumors obtained from patients with colon cancer showed higher levels of ORAI1/3 and HIF-1/2 α than the adjacent colon tissues (Fig. 1C and D).

Elevated ORAI1/3 and HIF-1/2 α as well as SOCC under hypoxia

To mimic the hypoxic tumor microenvironment, we checked the protein levels of ORAI1/3 and HIF-1/2 α in response to prolonged hypoxia in CW-2 cells. ORAI1/3 and HIF-1/2 α expression was significantly exacerbated under hypoxia in CW-2 cells (Fig. 1E, F). Moreover, hypoxia also



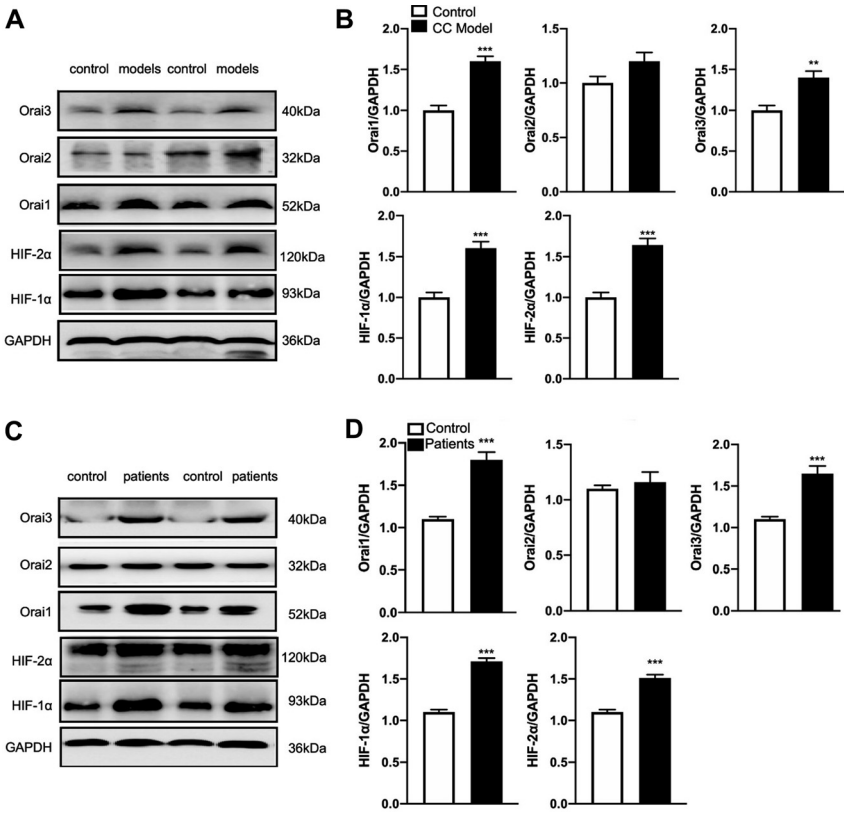


Fig. 1. Upregulation of ORAI1/3 and HIF-1/2α in colon cancer.

(A) Original western blot showing the ORAI1/2/3 and HIF-1/2α proteins in the colon tumors and healthy colon tissues from xenograft models. (B) Arithmetic means \pm SEM ($n = 32$) showing the ORAI1/2/3 and HIF-1/2α proteins in the colon tumors and healthy colon tissues from xenograft models. (C) Original western blot showing the ORAI1/2/3 and HIF-1/2α proteins in the colon tumors from patients with colon cancer and adjacent tissue. (D) Arithmetic means \pm SEM ($n = 32$) showing the ORAI1/2/3 and HIF-1/2α proteins in the colon tumors from patients with colon cancer and adjacent tissue. (E) Original western blot ($n = 4$) showing the protein levels of ORAI1/3, and HIF-1/2α in CW-2 cells after hypoxia treatment for 12 h. (F) Arithmetic means \pm SEM ($n = 4$) showing the protein levels of ORAI1, ORAI3, and HIF-1/2α in CW-2 cells after hypoxia treatment for 12 h. (G) Arithmetic means (\pm SEM, $n = 7$) of fura-2 fluorescence-ratio before and following extracellular Ca^{2+} removal and addition of thapsigargin (1 μM), and re-addition of extracellular Ca^{2+} in CW-2 cells after hypoxia treatment for 12 h. (H) Arithmetic means (\pm SEM, $n = 7$) of fura-2 fluorescence-ratio before and following extracellular Ca^{2+} removal and addition of thapsigargin (1 μM), and re-addition of extracellular Ca^{2+} in *siOrai1* as well as *siNEG* CW-2 cells. (I) Arithmetic means (\pm SEM, $n = 7$) of fura-2 fluorescence-ratio before and following extracellular Ca^{2+} removal and addition of thapsigargin (1 μM), and re-addition of extracellular Ca^{2+} in *siOrai3* as well as *siNEG* CW-2 cells.

*** $P < 0.001$ indicates a statistically significant difference



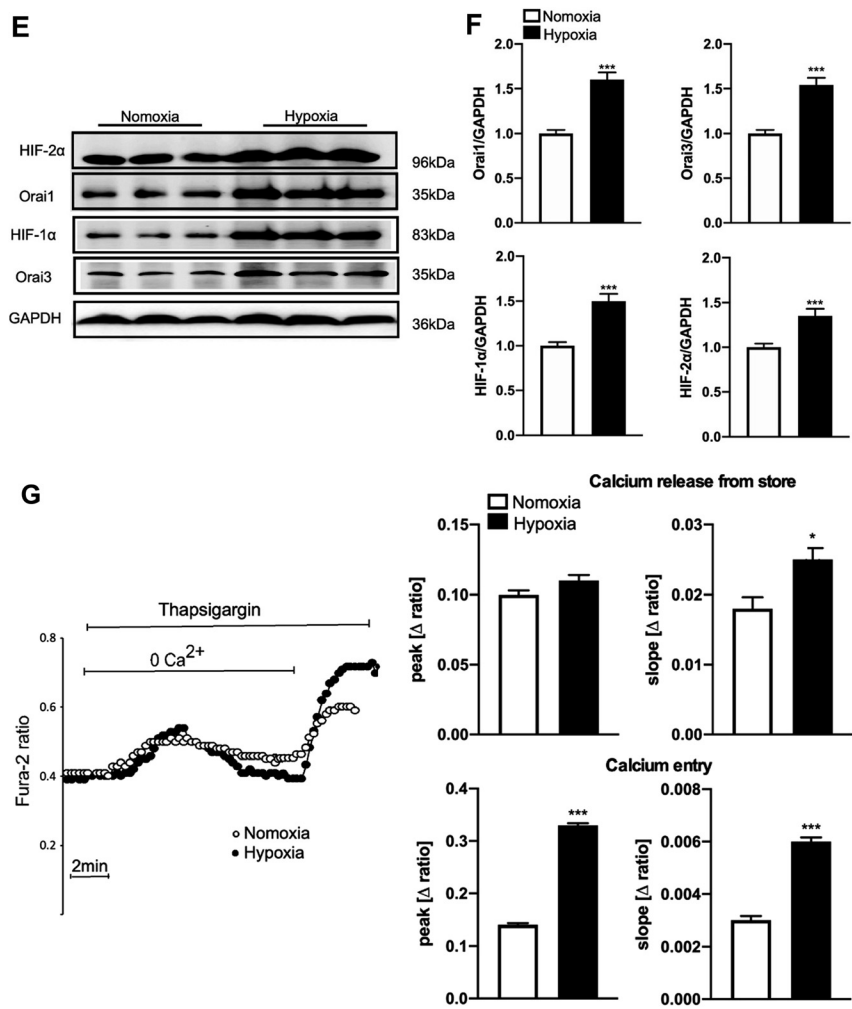


Fig. 1.



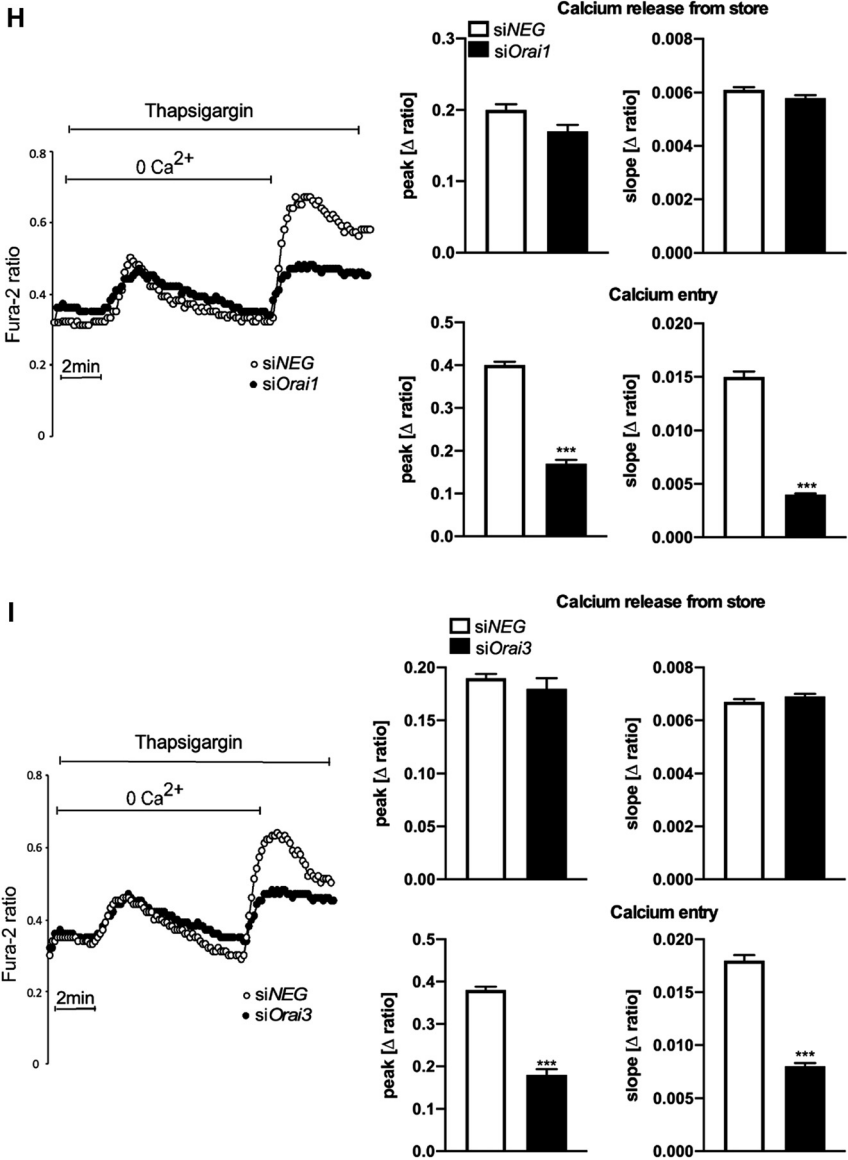


Fig. 1.

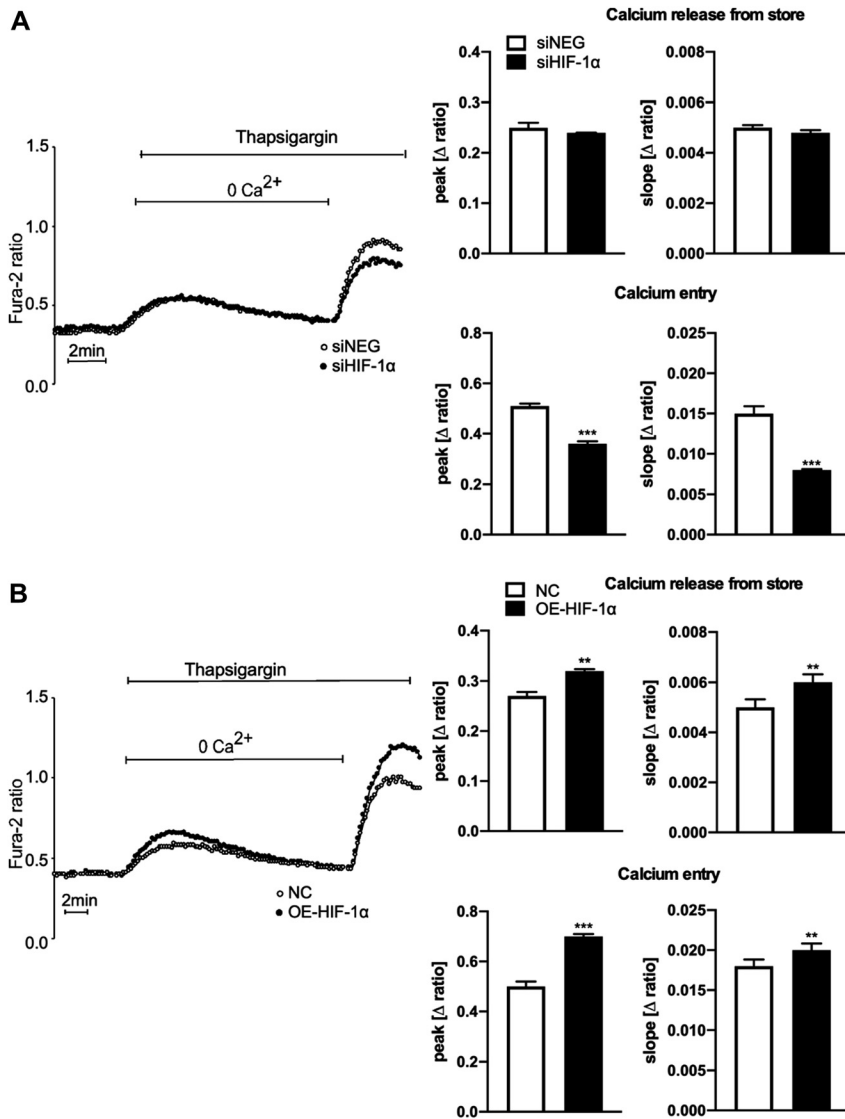


Fig. 2. Reduced SOCE activity in siHif-1/2α cells.

(A) Arithmetic means (\pm SEM, $n = 6$) of fura-2 fluorescence-ratio following extracellular Ca²⁺ removal and addition of thapsigargin (1 μ M), and re-addition of extracellular Ca²⁺ in *siNEG* cells and *siHif-1α* CW-2 cells. (B) Arithmetic means (\pm SEM, $n = 6$) of fura-2 following extracellular Ca²⁺ removal and addition of thapsigargin (1 μ M), and re-addition of extracellular Ca²⁺ in control and *OE-Hif-1α* CW-2 cells. (C) Arithmetic means (\pm SEM, $n = 6$) of fura-2 following extracellular Ca²⁺ removal and addition of thapsigargin (1 μ M), and re-addition of extracellular Ca²⁺ in *siNEG* cells and *siHif-2α* CW-2 cells. (D) Arithmetic means (\pm SEM, $n = 6$) of fura-2 following extracellular Ca²⁺ removal and addition of thapsigargin (1 μ M), and re-addition of extracellular Ca²⁺ in control and *OE-Hif-2α* CW-2 cells.

**** $P < 0.001$ indicate a statistically significant difference



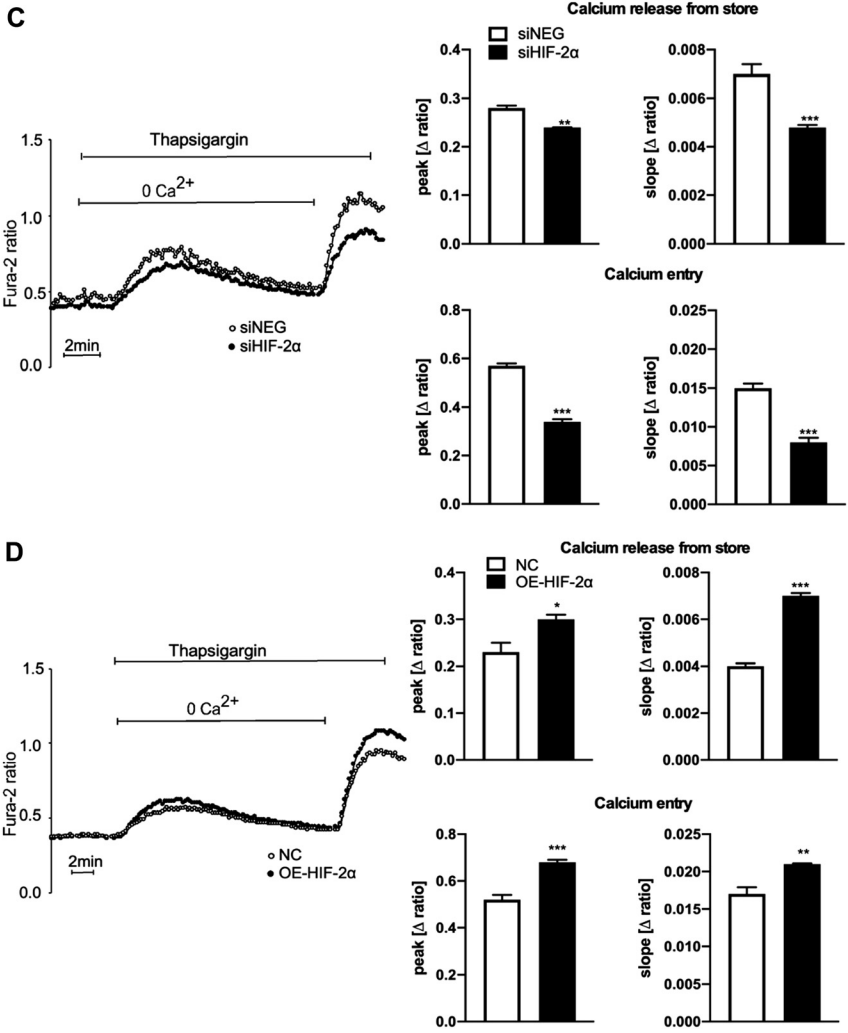


Fig. 2.



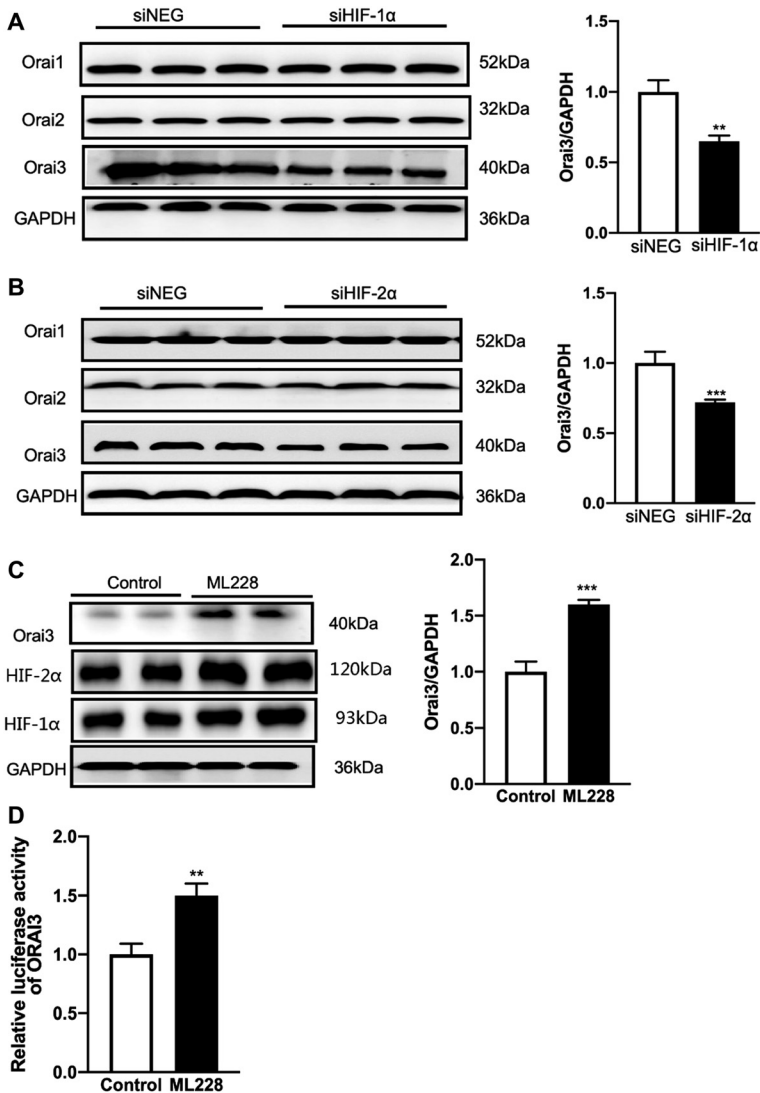


Fig. 3. HIF-1/2α silencing specifically decreased ORAI3.

(A) Original western blot and arithmetic means \pm SEM ($n = 5$) showing ORAI1, ORAI2, and ORAI3 protein expression in *siHif-1α* CW-2 cells. (B) Original western blot and arithmetic means \pm SEM ($n = 5$) showing ORAI1, ORAI2, and ORAI3 protein expression in *siHif-2α* CW-2 cells. (C) Original western blot and arithmetic means \pm SEM ($n = 5$) showing ORAI3 protein expression in the presence of ML228 (5 μ M) in CW-2 cells. (D) Arithmetic means \pm SEM ($n = 4$) of the trans-activity of ORAI3 in the presence of ML228 (5 μ M) in CW-2 cells.

*** $P < 0.001$ indicates a statistically significant difference

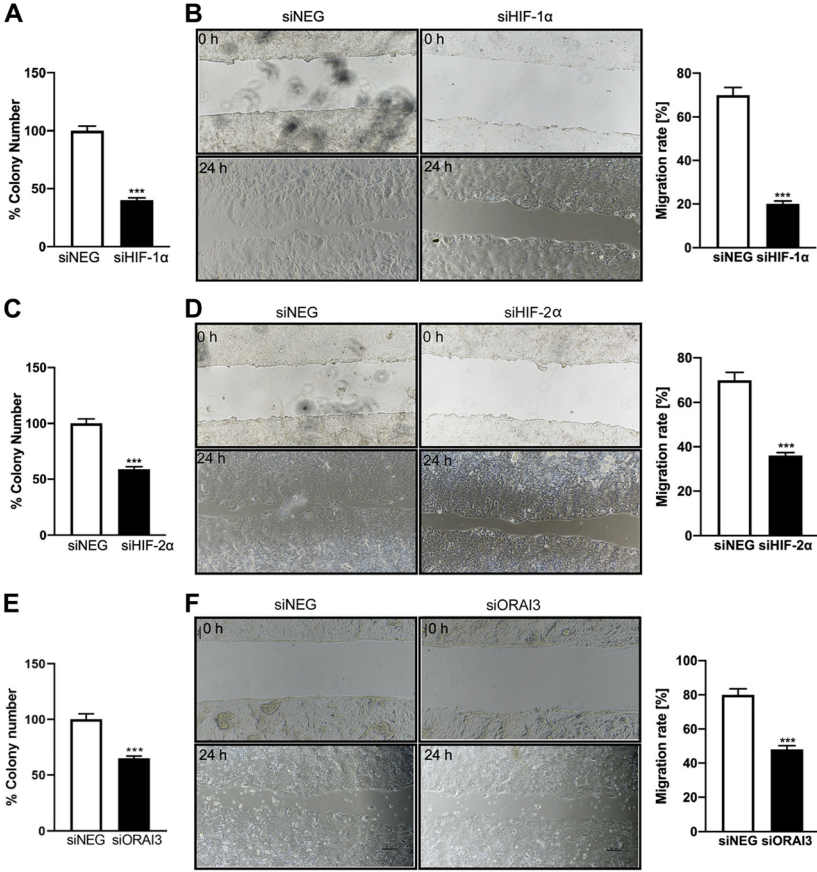


Fig. 4. HIF-1/2α-enhanced carcinoma phenotypes are ORAI3 sensitive.

(A) Arithmetic means \pm SEM ($n = 5$) of colony formation by *siHif-1α* CW-2 cells. (B) Original images and arithmetic means \pm SEM ($n = 5$) of migration of *siHif-1α* CW-2 cells in scratch assay. (C) Arithmetic means \pm SEM ($n = 5$) of colony formation by *siHIF-2α* CW-2 cells. (D) Original images and arithmetic means \pm SEM ($n = 5$) of migration of *siHif-2α* CW-2 cells in scratch assay. (E) Arithmetic means \pm SEM ($n = 5$) of colony formation by *siNEG* and *siOrai3* cells. (F) Original images and arithmetic means \pm SEM ($n = 5$) of the migration in *siNEG* and *siOrai3* cells. (G) Arithmetic means \pm SEM ($n = 5$) of colony formation by *siNEG* and *siOrai3* cells in the presence of ML228 (5 μ M) for 12 h. (H) Original images and arithmetic means \pm SEM ($n = 5$) of the migration in *siOrai3* cells in the presence of ML228 (5 μ M) for 12 h. (I) Arithmetic means \pm SEM ($n = 12$) of tumor volumes in *shNEG* and *shOrai3* nude mice.

*** $P < 0.001$ indicates a statistically significant difference

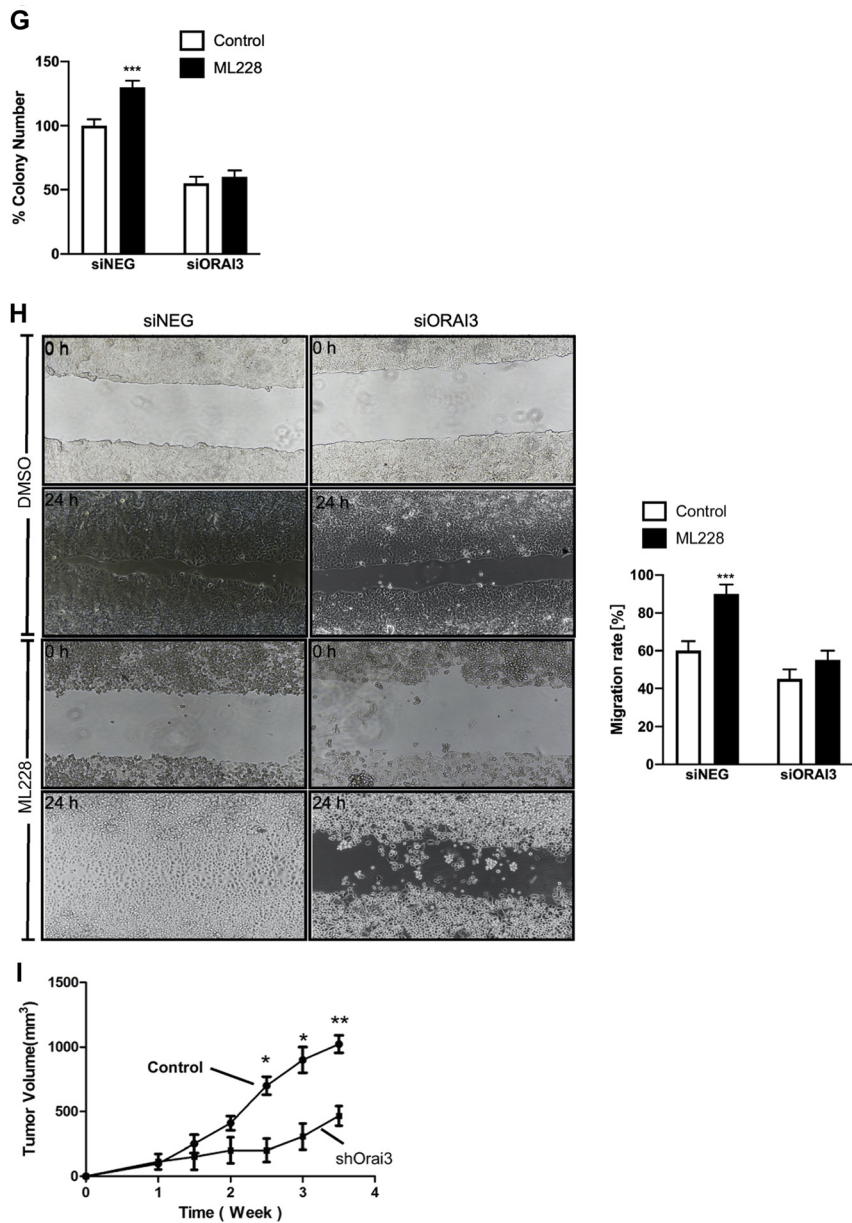


Fig. 4.



considerably increased SOCE, including Ca^{2+} released from store and Ca^{2+} entry (Fig. 1G). Additionally, both *ORAI1* and *ORAI3* silencing significantly suppressed Ca^{2+} entry in CW-2 cells (Fig. 1H and I), whereas *ORAI2* knock-down had no observable effect on SOCE (data not shown).

SOCC activity is HIF-1/2 α dependent in CW-2 cells

To examine the specific role of each *HIF* homolog in SOCE, we manipulated the expression of HIF-1 α and HIF-2 α in CW-2 cells. SOCE activity was decreased in *siHIF-1 α* cells (Fig. 2A). The peak and slope representing SOCE were significantly lower in *siHIF-1 α* cells than those in *siNEG* cells. Meanwhile, *HIF-1 α* was overexpressed (termed over-expression cells, *OE-HIF-1 α* , and virus-negative control, NC). As illustrated in Fig. 2B, SOCE activity was higher in *OE-HIF-1 α* cells than in NC cells. Similarly, *siHIF-2 α* cells showed lower SOCC activity than *siNEG* cells (Fig. 2C), whereas *OE-HIF-2 α* cells displayed higher SOCC activity than NC cells (Fig. 2D). The findings above indicate that both HIF-1 α and HIF-2 α contribute to SOCE.

To identify the components of SOCE regulated by HIF-1/2 α , *ORAI1/2/3* expression was quantified by western blot. *ORAI3* expression was significantly decreased in *siHIF-1/2 α* cells (Fig. 3A and B), and enhanced by ML228 treatment (Fig. 3C). HIF-1 α deletion did not affect the levels of *ORAI1* and *ORAI2* (Fig. 2). Moreover, we utilized a pGL3-*ORAI3*-3'-UTR luciferase reporter vector to check whether *ORAI3* transcription was regulated by HIFs. As shown in Fig. 3D, ML228 treatment dramatically increased the transcription of *ORAI3*, which reflected that *HIF-1/2 α* facilitated *ORAI3* at the transcriptional level.

Role of HIF-1/2 α in colon cancer is *ORAI3*-dependent

siHIF-1 α and *siHIF-2 α* deficiency inhibited colony-forming potential and cell migration capacity (Fig. 4A–D). Moreover, ML228 enhanced colony-forming potential and migration capacity, and these effects could be abolished by *ORAI3* silencing (Fig. 4E and F). Ultimately, *ORAI3* knockdown markedly suppressed the tumor volume of colon cancer xenograft models (Fig. 4G and I).

DISCUSSION

We explored the role of HIF-1/2 α in colon cancer and demonstrated the involvement of *ORAI3* in the process. It is generally accepted that SOCE, whose inhibition reduces tumor size in breast cancer as well as esophageal cancer [15] is related to carcinogenesis. STIM1 and *ORAI1*, the major components of SOCE are overexpressed in a wide variety of cancers [15, 30–32]. Yet for a long time there has been a debate as to whether or not SOCE can be modulated by a pathway involving *ORAI3*. We confirmed that both *ORAI1* and *ORAI3* deficiency decreased SOCE in CW-2 cells. There is a growing appreciation for the involvement of *ORAI3* rather than *ORAI1* in carcinogenesis [33, 34]. Herein, we observed the enhanced expression of *ORAI1* and *ORAI3* in colon cancer patients and mice models, and found that *ORAI3* deficiency led to a significant reduction of the colon tumor volume *in vivo* and the migration capacity *in vitro*.

As for the modulation of *ORAI3*, Motiani et al. proposed that ER α silencing significantly reduces *ORAI3* level by 42% in breast cancer [21], indicating the regulatory role of ER α in *ORAI3* and reflecting the existence of additional *Orai3* regulatory mechanisms. Azimi et al. clearly reported



increased ORAI3 involving the HIF-1 α pathway in breast cancer cells [25]. We found that that HIF-2 α and HIF-1 α are equally important for ORAI3 expression in colon cancer.

HIFs are intrinsic markers of tumor hypoxia and are pivotal for tumor angiogenesis and growth. Enhanced expression of HIF-1/2 α is associated with cancer progression including colorectal cancer [27, 28]. Zhu et al. suggest that *HIF-1 α* directly controls *Stim1* transcription and contributes to SOCE under hypoxia [35]. Meanwhile, as described by Azimi (2019), HIF-1 α increases the ORAI3 level in breast cancer cells [25], which is consistent with our results in CW-2 cells. Moreover, the luciferase assay identified the linkage between ORAI3 and HIF-1/2 α . Nevertheless, Wang et al. found that exposure to chronic hypoxia enhanced the levels of both ORAI1 and ORAI2 but not ORAI3 in pulmonary arterial smooth muscle cells (PASMs) [36]. This discrepancy might be attributed to the excitable cell type of PASMs and the limited expression of ORAI3. PASMs belong to excitable cells that are mainly triggered by L-type calcium channel, and ORAI3 preferentially exists in tumor cells.

There has been a long-term interest in distinguishing the roles of HIF-1 α and HIF-2 α . HIF-1 α and HIF-2 α share very similar characteristics and regulate many common genes, whereas the expression of HIF-2 α is restricted to the lung, heart and gut [26]. HIF-2 α preferentially regulates genes important for tumor growth and cell cycle progression [37]. According to Maranchie (2002), HIF-2 α (and not HIF-1 α) promotes tumor growth in a renal carcinoma xenograft model [38]. We found that the migration and colony formation of CW-2 cells were inhibited by both *HIF-1 α* and *HIF-2 α* silencing. Notwithstanding its limitations, such data provide an impetus for considering the HIFs-ORAI3 axis as a potential target for colon cancer therapy.

In this study, we provide evidence supporting the notion that both HIF-1 α and HIF-2 α contribute to the migration of colon cancer and facilitate tumor formation by specifically recruiting ORAI3, highlighting a critical relationship of HIF-1/2 α and ORAI3.

Conflicts of interest: All authors disclose that they do not have any potential conflicts of interest.

Data availability statement: Data available on request from the authors.

ACKNOWLEDGMENTS

This study was supported by the National Natural Science Foundation of China (Grant No. 31801172), and the Young Talent Project of Henan Province of China (2019HYTP031).

REFERENCES

1. Semenza GL. Hypoxia-inducible factors in physiology and medicine. *Cell* 2012; 148: 399–408.
2. Pugh CW, Ratcliffe PJ. Regulation of angiogenesis by hypoxia: role of the HIF system. *Nat Med* 2003; 9: 677–84.
3. Manalo DJ, Rowan A, Lavoie T, Natarajan L, Kelly BD, Ye SQ, et al. Transcriptional regulation of vascular endothelial cell responses to hypoxia by HIF-1. *Blood* 2005; 105: 659–69.



4. Yang X, Yin H, Zhang Y, Li X, Tong H, Zeng Y, et al. Hypoxia-induced autophagy promotes gemcitabine resistance in human bladder cancer cells through hypoxia-inducible factor 1alpha activation. *Int J Oncol* 2018; 53: 215–24.
5. Cesario JM, Brito RB, Malta CS, Silva CS, Matos YS, Kunz TC, et al. A simple method to induce hypoxia-induced vascular endothelial growth factor-A (VEGF-A) expression in T24 human bladder cancer cells. *In Vitro Cell Dev Biol Anim* 2017; 53: 272–76.
6. Onita T, Ji PG, Xuan JW, Sakai H, Kanetake H, Maxwell PH, et al. Hypoxia-induced, perinecrotic expression of endothelial Per-ARNT-Sim domain protein-1/hypoxia-inducible factor-2alpha correlates with tumor progression, vascularization, and focal macrophage infiltration in bladder cancer. *Clin Cancer Res* 2002; 8: 471–80.
7. Prevarskaya N, Ouadid-Ahidouch H, Skryma R, Shuba Y. Remodelling of Ca^{2+} transport in cancer: how it contributes to cancer hallmarks? *Philos Trans R Soc Lond B Biol Sci* 2014; 369: 20130097.
8. Roderick HL, Cook SJ. Ca^{2+} signalling checkpoints in cancer: remodelling Ca^{2+} for cancer cell proliferation and survival. *Nat Rev Cancer* 2008; 8: 361–75.
9. Yan J, Fu Z, Zhang L, Li C. Orai1 is involved in leptin-sensitive cell maturation in mouse dendritic cells. *Biochem Biophys Res Commun* 2018; 503: 1747–53.
10. Prakriya M, Feske S, Gwack Y, Srikanth S, Rao A, Hogan PG. Orai1 is an essential pore subunit of the CRAC channel. *Nature* 2006; 443: 230–3.
11. Putney JW, Jr. New molecular players in capacitative Ca^{2+} entry. *J Cell Sci* 2007; 120: 1959–65.
12. Yan J, Zhao W, Gao C, Liu X, Zhao X, Wei T, et al. Leucine-rich repeat kinase 2 regulates mouse dendritic cell migration by ORAI2. *FASEB J* 2019; 33: 9775–84.
13. Huang GN, Zeng W, Kim JY, Yuan JP, Han L, Muallem S, et al. STIM1 carboxyl-terminus activates native SOC, I(crac) and TRPC1 channels. *Nat Cell Biol* 2006; 8: 1003–10.
14. Yang S, Zhang JJ, Huang XY. Orai1 and STIM1 are critical for breast tumor cell migration and metastasis. *Cancer Cell* 2009; 15: 124–34.
15. Chen YF, Chiu WT, Chen YT, Lin PY, Huang HJ, Chou CY, et al. Calcium store sensor stromal-interaction molecule 1-dependent signaling plays an important role in cervical cancer growth, migration, and angiogenesis. *Proc Natl Acad Sci U S A* 2011; 108: 15225–30.
16. Flourakis M, Lehen'kyi V, Beck B, Raphael M, Vandenberghe M, Abeele FV, et al. Orai1 contributes to the establishment of an apoptosis-resistant phenotype in prostate cancer cells. *Cell Death Dis* 2010; 1: e75.
17. Enfissi A, Prigent S, Colosetti P, Capiod T. The blocking of capacitative calcium entry by 2-aminoethyl diphenylborate (2-APB) and carboxyamidotriazole (CAI) inhibits proliferation in Hep G2 and Huh-7 human hepatoma cells. *Cell Calcium* 2004; 36: 459–67.
18. Padar S, Bose DD, Livesey JC, Thomas DW. 2-Aminoethoxydiphenyl borate perturbs hormone-sensitive calcium stores and blocks store-operated calcium influx pathways independent of cytoskeletal disruption in human A549 lung cancer cells. *Biochem Pharmacol* 2005; 69: 1177–86.
19. Vashisht A, Trebak M, Motiani RK. STIM and Orai proteins as novel targets for cancer therapy. A Review in the theme: cell and molecular processes in cancer metastasis. *Am J Physiol Cell Physiol* 2015; 309: C457–69.
20. Gui L, Wang Z, Han J, Ma H, Li Z. High expression of Orai1 enhances cell proliferation and is associated with poor prognosis in human colorectal cancer. *Clin Lab* 2016; 62: 1689–98.
21. Motiani RK, Zhang X, Harmon KE, Keller RS, Matrougui K, Bennett JA, et al. Orai3 is an estrogen receptor alpha-regulated Ca^{2+} channel that promotes tumorigenesis. *FASEB J* 2013; 27: 63–75.
22. Shuttleworth TJ. Orai3 – the ‘exceptional’ Orai? *J Physiol* 2012; 590: 241–57.
23. Tanwar J, Arora S, Motiani RK. Orai3: oncochannel with therapeutic potential. *Cell Calcium* 2020; 90: 102247.



24. Motiani RK, Abdullaev IF, Trebak M. A novel native store-operated calcium channel encoded by Orai3: selective requirement of Orai3 versus Orai1 in estrogen receptor-positive versus estrogen receptor-negative breast cancer cells. *J Biol Chem* 2010; 285: 19173–83.
25. Azimi I, Milevskiy MJG, Chalmers SB, Yapa K, Robitaille M, Henry C, et al. ORAI1 and ORAI3 in breast cancer molecular subtypes and the identification of ORAI3 as a hypoxia sensitive gene and a regulator of hypoxia responses. *Cancers (Basel)* 2019; 11: 208.
26. Wiesener MS, Jurgensen JS, Rosenberger C, Scholze CK, Horstrup JH, Warnecke C, et al. Widespread hypoxia-inducible expression of HIF-2alpha in distinct cell populations of different organs. *FASEB J* 2003; 17: 271–3.
27. Burkitt K, Chun SY, Dang DT, Dang LH. Targeting both HIF-1 and HIF-2 in human colon cancer cells improves tumor response to sunitinib treatment. *Mol Cancer Ther* 2009; 8: 1148–56.
28. Yoshimura H, Dhar DK, Kohno H, Kubota H, Fujii T, Ueda S, et al. Prognostic impact of hypoxia-inducible factors 1alpha and 2alpha in colorectal cancer patients: correlation with tumor angiogenesis and cyclooxygenase-2 expression. *Clin Cancer Res* 2004; 10: 8554–60.
29. Theriault JR, Perez J, Gilbert S, Palmer M, Schreiber SL, Lindsley CW, et al. Discovery of a small molecule activator of the hypoxia inducible factor pathway. In: *Probe reports from the NIH molecular libraries program*. Bethesda (MD): National Center for Biotechnology Information (US); 2010.
30. Villalobos C, Hernandez-Morales M, Gutierrez LG, Nunez L. TRPC1 and ORAI1 channels in colon cancer. *Cell Calcium* 2019; 81: 59–66.
31. Abdelazeem KNM, Droppova B, Sukkar B, Al-Maghout T, Pelzl L, Zacharopoulou N, et al. Upregulation of Orai1 and STIM1 expression as well as store-operated Ca(2+) entry in ovary carcinoma cells by placental growth factor. *Biochem Biophys Res Commun* 2019; 512: 467–72.
32. Cantonero C, Sanchez-Collado J, Gonzalez-Nunez MA, Salido GM, Lopez JJ, Jardin I, et al. Store-independent Orai1-mediated Ca(2+) entry and cancer. *Cell Calcium* 2019; 80: 1–7.
33. Benzerdjeb N, Sevestre H, Ahidouch A, Ouadid-Ahidouch H. Orai3 is a predictive marker of metastasis and survival in resectable lung adenocarcinoma. *Oncotarget* 2016; 7: 81588–97.
34. Vashisht A, Tanwar J, Motiani RK. Regulation of proto-oncogene Orai3 by miR18a/b and miR34a. *Cell Calcium* 2018; 75: 101–11.
35. Li Y, Guo B, Xie Q, Ye D, Zhang D, Zhu Y, et al. STIM1 mediates hypoxia-driven hepatocarcinogenesis via interaction with HIF-1. *Cell Rep* 2015; 12: 388–95.
36. Wang J, Xu C, Zheng Q, Yang K, Lai N, Wang T, et al. Orai1, 2, 3 and STIM1 promote store-operated calcium entry in pulmonary arterial smooth muscle cells. *Cell Death Discov* 2017; 3: 17074.
37. Hu CJ, Wang LY, Chodosh LA, Keith B, Simon MC. Differential roles of hypoxia-inducible factor 1alpha (HIF-1alpha) and HIF-2alpha in hypoxic gene regulation. *Mol Cell Biol* 2003; 23: 9361–74.
38. Maranchie JK, Vasselli JR, Riss J, Bonifacio JS, Linehan WM, Klausner RD. The contribution of VHL substrate binding and HIF1-alpha to the phenotype of VHL loss in renal cell carcinoma. *Cancer Cell* 2002; 1: 247–55.

